JOURNAL OF SOLID STATE CHEMISTRY **136,** 221–226 (1998)
ARTICLE NO. SC977684

Bonding and Site Preferences in the New Quasi-Binary $Zr_{2.7}Hf_{11.3}P_9$

Holger Kleinke[1] and Hugo F. Franzen

Ames Laboratory—Department of Energy, Iowa State University, Ames, Iowa 50011

Received June 30, 1997; in revised form October 20, 1997; accepted October 30, 1997

The new quasi-binary $Zr_{2.7}Hf_{11.3}P_9$ was synthesized by arc-melting of Zr, Hf, Co, and HfP in a ratio corresponding to the initial composition "$Zr_{2.25}Hf_{6.75}Co_2P_4$". $Zr_{2.7}Hf_{11.3}P_9$ crystallizes in the $Zr_{14}P_9$ structure type, which is unknown in the binary Hf/P system. The ideal orthorhombic lattice dimensions (space group *Pnnm* (No. 58), $Z = 4$) were refined to $a = 16.640(7)$ Å, $b = 27.40(2)$ Å, $c = 3.619(1)$ Å, $V = 1650(2)$ Å^3. The structure consists of three-dimensional condensed one-, two-, and three-capped trigonal (Zr, Hf)$_6$P prisms, occurring with numerous short *M*–*M* bonds (*M* = Zr, Hf). Each of the 15 metal sites is statistically occupied by a mixture of Zr and Hf, which varies significantly from site to site. The Hf/Zr ratio in a given site depends on the *M*–*M* and *M*–P interactions. The systematic increase of this ratio with increasing total bond order, as evaluated via Mulliken overlap populations and Pauling bond orders, can be understood based on the trend that Hf forms stronger *M*–*M* and *M*–P bonds than Zr. As expected for a metal-rich phosphide, band structure calculations for the hypothetical "$Hf_{14}P_9$" carried out with the extended Hückel approximation result in a significant density of states at the Fermi level. © 1998 Academic Press

Key Words: **zirconium hafnium phosphide; structure and bonding; site preferences.**

INTRODUCTION

Earlier investigations in the quasi-binary Nb/Ta/S system led to the synthesis of new compounds, forming new structure types. Although Nb and Ta are closely related metal atoms, none of the four quasi-binary sulphides $Nb_{1.72}Ta_{3.28}S_2$ (1), $Nb_{0.95}Ta_{1.05}S$ (2), $Nb_{4.92}Ta_{6.08}S_4$ (3), and $Nb_{6.74}Ta_{5.26}S_4$ (4) has a counterpart among the binaries. The concept of differential fractional site occupancies (DFSO) has been used to explain the formation of new structure types in quasi-binary and more recently, quasi-ternary systems, as well as the differing site preferences of the different atom species. Further examples include the phosphides $Zr_{6.45}Nb_{4.55}P_4$ (5) and $Hf_{5.08}Mo_{0.92}P_3$ (6), and most recently the quasi-ternary $Hf_5Nb_5Ni_3P_5$ (7). On the other hand, complete ordering on the metal sites was observed for the isostructural ZrNbP and HfNbP (Co_2Si type) (8).

In general, DFSO stabilized materials have three common features: (i) the metal atom sites are statistically occupied by two different metal atoms; (ii) the ratio of the metals per site varies only insignificantly, but differs from one site to another; and (iii) no binary isostructural compounds occur. From that point of view, $Zr_{2.7}Hf_{11.3}P_9$ is not a DFSO stabilized compound, because it is isostructural with $Zr_{14}P_9$ (9). On the other hand, 80.7% of the metal atoms in $Zr_{2.7}Hf_{11.3}P_9$ are Hf, and a "$Hf_{14}P_9$" has not yet been found.

However, $Zr_{2.7}Hf_{11.3}P_9$ is the first report of a mixed Zr/Hf compound where systematic site preferences are observed. No systematic trend has been found for the solution of Hf in Zr_2S (10), which might be due to the fact that investigation (11) emphasized metal–metal interactions and neglected the metal-nonmetal interactions. To explain the site preferences observed in $Zr_{2.7}Hf_{11.3}P_9$, it is necessary to consider both metal–metal and metal-nonmetal interactions, which will be discussed in this article.

EXPERIMENTAL

Synthesis

To prevent vaporization of elemental phosphorus during arc-melting, HfP was previously prepared in a fused silica tube at 800°C, starting with the elements in the stoichiometric ratio (Hf: ALFA AESAR, powder, −325 mesh, purity 99.6% (containing 2–3.5% Zr); P: ALFA AESAR, powder, −100 mesh, red amorphous, 99%). In an attempt to replace Zr in $Zr_9Co_2P_4$ (12) by Hf, we cold-pressed a mixture of HfP, Zr (ALFA AESAR, powder, −20 + 60 mesh, purity 99.7% (Hf impurity: 97 ppm)), Hf and Co (ALFA AESAR, powder, −50 + 150 mesh, 99.9%) in a ratio of 4 : 2.25 : 2.75 : 2, which corresponds to the starting composition "$Zr_{2.25}Hf_{6.75}Co_2P_4$". This pellet was arc-melted twice after inversion under a slight over-pressure of a dynamic argon flow. Since the powder diagram obtained from the bulk sample could not be identified at that time, we annealed this sample at 1500°C in an induction furnace

[1]Current address: Philipps-Universität Marburg, Fb Chemie, D-35032 Marburg, Germany.

0022-4596/98 $25.00

under a dynamic vacuum of approximately 10^{-6} bar. After solving the structure of a single crystal selected from the annealed sample, we could reproduce $Zr_{2.7}Hf_{11.3}P_9$ starting from the corresponding stoichiometric mixture of Zr, Hf, and HfP, showing that the presence of Co is not necessary for the formation of $Zr_{2.7}Hf_{11.3}P_9$.

Structure Determination

A prismatic shaped crystal was selected for the single crystal structure determination. The data collection was carried out using the automatic four-circle Rigaku AFC6R diffractometer, equipped with graphite monochromatized MoK_α radiation and a 12 KW rotating anode. The orientation matrix and the cell constants were obtained after least-square refinements of 25 carefully refined reflections in the range of $15.1^\circ < 2\theta < 22.6^\circ$. The observed intensities were corrected for Lorentz and polarization effects. The refinements were performed using the TEXSAN program package (13).

The structure model with the positional parameters of $Zr_{14}P_9$, as given in Pearson's handbook for intermetallic phases (14), refined to different negative temperature factors for the Zr atoms. Using the program SHELXL93 for the refinement, which does not allow negative temperature factors, the isotropic displacements of the Zr atoms resulted in a wide range (between $U_{eq} = 0.0002(6)$ Å^2 and $U_{eq} = 0.0071(5)$ Å^2). In addition, the residual factors were too high (R(F) = 0.0582), as were the temperature factors of the P atoms ($U_{eq} > 0.04$ Å^2). Similarly, a refinement of the model '$Hf_{14}P_9$' resulted in a range of temperature factors between 0.0032(5) Å^2 and 0.0105(4) Å^2 for the metal atoms and minimal temperature factors of the P atoms (*i.e.*, $U_{eq} = 0.00001$ Å^2). For these reasons, we assumed fractional Zr/Hf occupancies for all metal sites. A refinement with a constant Zr/Hf ratio for all metal sites yielded $R(F) = 0.0462$, but again the range of temperature factors of the metal sites was fairly large, varying from 0.0032(5) to 0.0105(4) Å^2. The assumption of partial ordering, *i.e.*, refining independently the occupancy factor of all the metal sites, yielded more uniform temperature factors and a lower residual value of R(F) = 0.0453. Refining this model with anisotropic temperature factors for the metal positions, carried out against F^2, resulted in final residual factors of $R(F^2) = 0.072$ and $R_w(F^2) = 0.083$ (R(F) = 0.044). The stoichiometry was refined to $Zr_{2.7(1)}Hf_{11.3(1)}P_9$. Crystallographic details can be found in Table 1. Atomic positions, equivalent temperature factors, and fractional site occupancies are given in Table 2, interatomic distances in Table 3.

TABLE 1
Selected Crystallographic Data for $Zr_{2.7(1)}Hf_{11.3(1)}P_9$

Empirical formula	$Zr_{2.7}Hf_{11.3}P_9$
Molecular weight	2542.9 g/mol
Temperature of data collection	295 K
Crystal dimensions	0.03 mm × 0.02 mm × 0.002 mm
Space group	*Pnnm* (No. 68)
Unit cell dimensions	$a = 16.640(7)$ Å, $b = 27.40(2)$ Å, $c = 3.619(1)$ Å, $V = 1650(2)$ Å^3
Number of formula units	4
Calculated density	10.24 g/cm^3
Absorption coefficient	72.6 mm^{-1}
F(000)	4227
Scan mode, scan width	ω, $(0.85 + 0.34 \tan\theta)^\circ$
Scan speed	8.0°/min (in ω, 3 rescans)
Range of 2θ	4°–70°
No. of measured reflections	7613
No. of independent reflections	4290 ($R_{int} = 0.105$)
No. of observed reflections ($I > 3\sigma(I)$)	1285
No. of parameters refined	129
$R(F^2)$, $R_w(F^2)$, goodness of fit (GOF)	0.072, 0.083, 1.10
Extinction coefficient	0.222663×10^{-7}
Max, min peak in final diff. map	4.18 e$^-$/Å^3, −4.81 e$^-$/Å^3
Absorption correction	DIFABS
Min, max transmission	0.80–1.63

RESULTS AND DISCUSSION

$Zr_{2.7}Hf_{11.3}P_9$ crystallizes in the $Zr_{14}P_9$ structure type. This is somewhat surprising considering the large Hf/Zr ratio of 4.2 and the fact that "$Hf_{14}P_9$" is unknown. Instead, Hf forms Hf_3P_2 (15) at a similar composition, which does not occur in the Zr–P phase diagram. The structure of $Zr_{2.7}Hf_{11.3}P_9$ contains M_6P prisms, single-, two-, and three-capped by M atoms, which are interconnected via common M atoms to a three-dimensional network (M = Zr, Hf). Numerous short M–M bonds occur in this structure, as emphasized in Fig. 1, but no short P–P contacts <3.5 Å are found. Only one M site ($M2$) is cubic coordinated by eight M atoms; all the other M coordination spheres are rather irregular. A more detailed structure description can be found in Ref. (9).

As expected because of the slightly different sizes of Zr and Hf (single bond radii according to Pauling: $r_{Zr} = 1.454$ Å, $r_{Hf} = 1.442$ Å (16)), all three axes of the unit cell of $Zr_{2.7}Hf_{11.3}P_9$ are shorter than those of the $Zr_{14}P_9$ cell. The differences vary from 0.4% (a axis) to 1.5% (c axis); the unit cell volume of $Zr_{2.7}Hf_{11.3}P_9$ is 2.6% smaller than that of $Zr_{14}P_9$. The decrease in the cell parameters occurs with an almost isotropic decrease of all interatomic distances. It is important to note that the labels used for the M sites in this article were taken from Pearson's handbook and thus are different than the notations in the original article (9). $M3$–$M13$ and all P atoms have the same numbers in both articles, but $M1$, $M2$, $M14$, and $M15$ correspond to Zr15, Zr14, Zr1, and Zr2, respectively. The shortest M–M distances in $Zr_{2.7}Hf_{11.3}P_9$ are $d_{M1-M11} = 3.017(2)$ Å, $d_{M2-M4} = 3.011(1)$ Å, and $d_{M2-M14} = 2.952(2)$ Å; the corresponding Zr–Zr distances in $Zr_{14}P_9$ are 3.027(2), 3.047(2), and

TABLE 2
Positional Parameters, Equivalent Temperature Factors, and Hf Occupancies for $Zr_{2.7(1)}Hf_{11.3(1)}P_9$

Atom	Site	x	y	z	B_{eq}/Å^2	% Hf
M1	2a	0	0	0	0.63(8)	99.6(1.2)
M2	2b	0	1/2	1/2	0.36(8)	78.8(1.2)
M3	4g	0.11873(8)	0.75486(6)	0	0.41(6)	76.0(1.0)
M4	4g	0.13558(8)	0.46942(5)	0	0.57(6)	84.2(1.0)
M5	4g	0.13664(8)	0.35361(6)	0	0.58(7)	74.8(1.0)
M6	4g	0.19924(8)	0.99060(6)	0	0.54(7)	74.4(1.0)
M7	4g	0.20226(8)	0.85687(6)	0	0.68(6)	85.2(1.0)
M8	4g	0.24628(8)	0.58374(5)	0	0.35(6)	73.6(1.0)
M9	4g	0.26656(9)	0.18732(5)	0	0.53(6)	82.6(1.0)
M10	4g	0.33359(8)	0.76256(5)	0	0.48(6)	84.8(1.0)
M11	4g	0.4293(1)	0.42309(6)	0	0.64(7)	73.8(1.0)
M12	4g	0.48012(8)	0.17685(5)	0	0.45(6)	80.2(1.0)
M13	4g	0.48568(8)	0.69691(5)	0	0.54(6)	85.8(1.0)
M14	4g	0.05043(8)	0.57944(5)	0	0.55(6)	85.2(1.0)
M15	4g	0.09751(9)	0.10435(6)	0	0.49(4)	77.2(1.0)
P1	4g	0.1333(4)	0.6571(3)	0	0.1(1)	
P2	4g	0.3426(4)	0.6650(3)	0	0.2(1)	
P3	4g	0.0497(5)	0.8553(3)	0	0.5(1)	
P4	4g	0.2671(4)	0.4218(3)	0	0.2(1)	
P5	4g	0.2742(5)	0.2856(3)	0	0.3(1)	
P6	4g	0.0480(4)	0.2675(3)	0	0.2(1)	
P7	4g	0.4365(4)	0.9099(3)	0	0.3(1)	
P8	4g	0.3466(4)	0.0383(3)	0	0.4(1)	
P9	4g	0.3972(4)	0.5329(3)	0	0.1(1)	

2.995(2) Å. Similarly, the shortest M–P distances in $Zr_{2.7}Hf_{11.3}P_9$ ($d_{M13-P2} = 2.537(2)$ Å and $d_{M14-P1} = 2.535(8)$ Å) are shorter than the corresponding Zr–P distances of 2.555(2) and 2.543(8) Å in $Zr_{14}P_9$. However, all these distances are close to the sums of the Pauling radii ($r_{Zr} = 1.454$ Å, $r_{Hf} = 1.442$ Å, and $r_P = 1.100$ Å (16)), implying strong bonding character.

Since no short P–P contacts occur in the structure of $Zr_{2.7}Hf_{11.3}P_9$, P can be considered as completely reduced to formal P^{3-}, which yields a formal ionic formulation of $(M^{1.93+})_{14}(P^{3-})_9$, *i.e.*, approximately two electrons are available for each M atom to form M–M bonds. According to our extended Hückel calculations (17, 18) of the electronic structure of $Zr_{2.7}Hf_{11.3}P_9$ using Hf parameters for all M sites, as obtained from solid state charge iteration on Hf_7P_4 (19) and the P parameters given by Clementi and Roetti (20) (see Table 4), the 3p block of phosphorus is located well below the Fermi level at −9.01 eV, *i.e.*, between −16 and −12 eV, separated from the partly filled d states of the Hf atoms, which occur above −11.5 eV. A significant density of states, mainly consisting of Hf states (Fig. 2), is found at the Fermi level. Considering the M–M bonds along all directions in the structure of $Zr_{2.7}Hf_{11.3}P_9$ and the number of d electrons available for M–M bonds, metallic properties can be assumed safely.

TABLE 3
Interatomic Distances [Å] for $Zr_{2.7}Hf_{11.3}P_9$

Atom	Atom	Distance	No.	Atom	Atom	Distance	No.
M1	M1	3.619(1)	2×	M7	P3	2.540(8)	
M1	M6	3.325(2)	2×	M7	P4	2.588(6)	2×
M1	M11	3.017(2)	4×	M7	P5	2.691(6)	2×
M1	M15	3.287(2)	2×	M8	M8	3.619(1)	2×
M1	P9	2.648(5)	4×	M8	M9	3.373(3)	2×
M2	M2	3.619(1)	2×	M8	M14	3.261(2)	2×
M2	M4	3.011(1)	4×	M8	M15	3.217(2)	
M2	M14	2.952(2)	4×	M8	P1	2.752(7)	
M2	P7	2.687(8)	2×	M8	P2	2.743(5)	
M2	P8	2.761(8)	2×	M8	P8	2.685(6)	2×
M3	M3	3.619(1)	2×	M8	P9	2.872(7)	
M3	M7	3.122(3)		M9	M9	3.619(1)	2×
M3	M9	3.216(2)	2×	M9	M10	3.210(2)	2×
M3	M10	3.582(2)		M9	M12	3.565(3)	
M3	M12	3.248(2)	2×	M9	M15	3.617(3)	
M3	M13	3.150(2)	2×	M9	P1	2.596(5)	2×
M3	P1	2.690(8)		M9	P2	2.636(5)	2×
M3	P3	2.984(9)		M9	P5	2.695(8)	
M3	P5	2.675(6)	2×	M10	M10	3.619(1)	2×
M3	P6	2.841(7)		M10	M12	3.516(2)	
M4	M4	3.619(1)	2×	M10	M13	3.105(2)	
M4	M5	3.173(3)		M10	P2	2.678(3)	
M4	M6	3.342(2)	2×	M10	P5	2.625(6)	2×
M4	M7	4.480(3)		M10	P6	2.679(5)	2×
M4	M8	3.634(3)		M11	M11	3.619(1)	2×
M4	M14	3.331(3)		M11	M13	3.580(3)	
M4	M14	3.372(2)		M11	M15	3.417(2)	2×
M4	P4	2.548(7)		M11	P3	2.616(6)	2×
M4	P7	2.716(6)	2×	M11	P4	2.700(7)	
M4	P8	2.632(6)	2×	M11	P9	3.055(8)	
M5	M5	3.619(1)	2×	M11	P9	3.129(7)	
M5	M7	3.236(2)	2×	M12	M12	3.619(1)	2×
M5	M10	3.122(2)	2×	M12	M13	3.505(3)	
M5	M12	3.279(2)	2×	M12	M14	3.265(2)	2×
M5	M14	3.613(2)		M12	P1	2.670(5)	2×
M5	P4	2.864(7)		M12	P6	2.622(6)	2×
M5	P5	2.953(8)		M12	P7	2.752(8)	
M5	P6	2.783(8)		M13	M13	3.619(1)	2×
M5	P7	2.670(6)	2×	M13	M15	3.409(2)	2×
M6	M6	3.619(1)	2×	M13	P2	2.537(7)	
M6	M7	3.665(4)		M13	P3	2.541(6)	2×
M6	M8	3.257(2)	2×	M13	P6	2.707(6)	2×
M6	M11	3.357(2)	2×	M14	M14	3.619(1)	2×
M6	M15	3.547(3)		M14	P1	2.535(8)	
M6	P4	2.673(6)	2×	M14	P7	2.638(6)	2×
M6	P8	2.779(8)		M14	P8	2.735(6)	2×
M6	P9	2.682(5)	2×	M15	M15	3.619(1)	2×
M7	M7	3.619(1)	2×	M15	P2	2.651(3)	2×
M7	M10	3.384(3)		M15	P3	2.686(8)	
M7	M11	3.370(2)	2×	M15	P9	2.668(6)	2×

The different site preferences for Nb and Ta in the niobium tantalum sulphides $Nb_{1.72}Ta_{3.28}S_2$ (1), $Nb_{0.95}Ta_{1.05}S$ (2), $Nb_{4.92}Ta_{6.08}S_4$ (3), and $Nb_{6.74}Ta_{5.26}S_4$ (4) can be understood based solely on the differences in M–M bonding between the metal sites (M = Nb, Ta). The Ta/Nb ratio

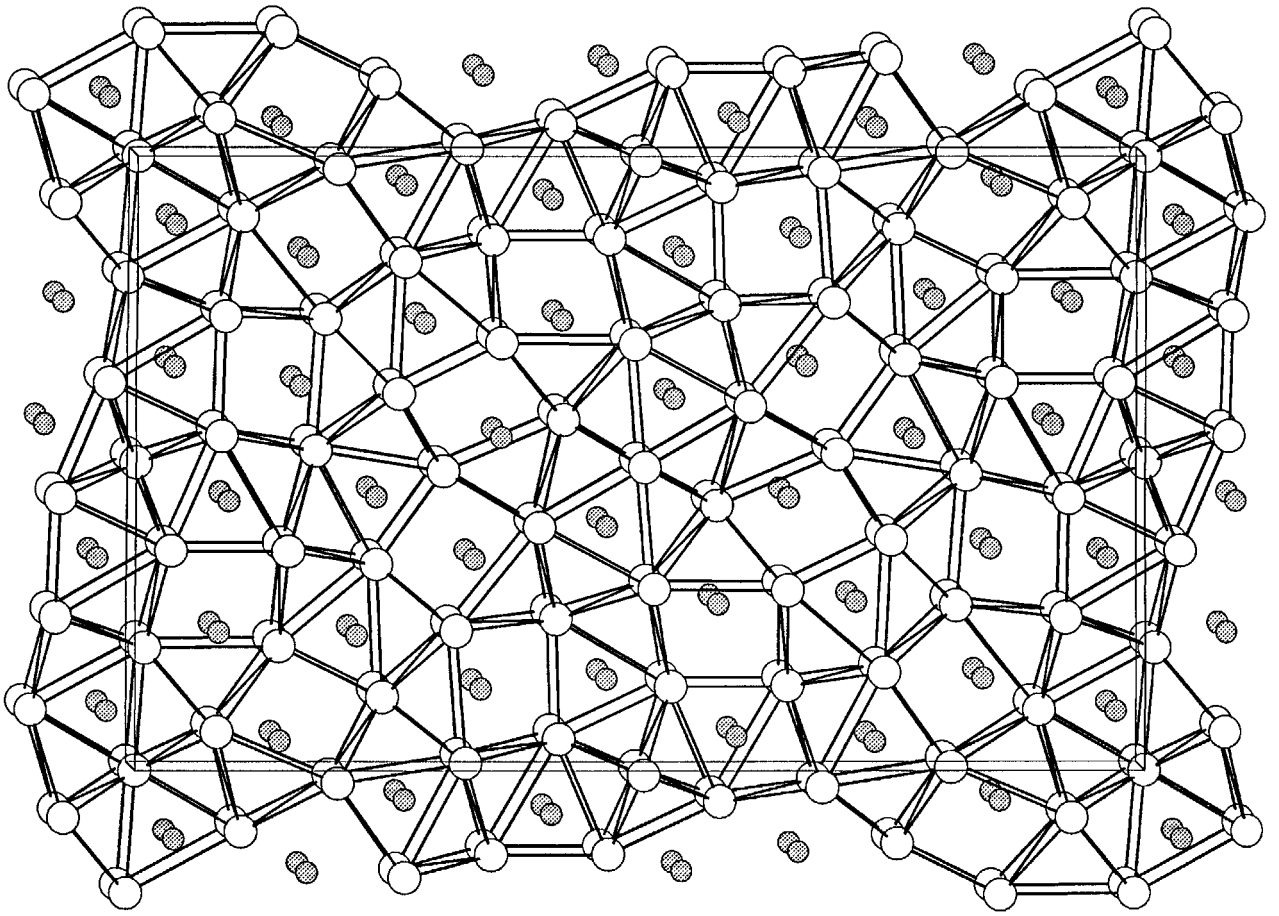

FIG. 1. Structure of $Zr_{2.7}Hf_{11.3}P_9$ in a projection along [001]. Vertical: *a* axis. Small, dotted circles represent P; large, white circles show Zr/Hf sites. Metal–P bonds are omitted for clarity.

increases with an increase in the *M*–*M* bond order, which can be determined by either the Pauling model or the Mulliken overlap populations using arbitrary units (21). The increase of the Ta/Nb ratio is due to the greater expansion of the 5*d* orbitals of Ta, compared to the 4*d* orbitals of Nb.

Since the metal/nonmetal ratio is much smaller in $Zr_{2.7}Hf_{11.3}P_9$ than in the sulphides mentioned above, the metal–nonmetal interaction might need to be included into the considerations of the different site preferences. We show the sums of the Pauling bond orders for the 15 metal sites as a function of Hf content in Fig. 3. (Using Pauling's equation $d(n) = d(1) - 0.6 \log n$, with n = bond order, $r_M = 1.442$ Å and $r_P = 1.100$ Å). The use of a fixed radius for all *M* sites is a good approximation because of the similar sizes of Zr and Hf and the relatively small range of the Hf/Zr ratio. If one concentrates only on the *M*–*M* or *M*–P interactions, it will be rather difficult to find a significant trend.

TABLE 4
Parameters Used for Extended Hückel Calculations

Orbital	H_{ii}/eV	ζ_1	c_1	ζ_2	c_2
Hf, 6*s*	−8.58	2.21			
Hf, 6*p*	−4.98	2.17			
Hf, 5*d*	−8.71	4.36	0.6967	1.709	0.5322
P, 3*s*	−18.60	1.88			
P, 3*p*	−12.50	1.63			

The linear fits of site occupation by Hf *vs* the *M*–*M* and *M*–P Pauling bond orders both have a positive slope, but the data for each scatter very much around the trendlines. Each minimum of the *M*–P bond orders corresponds to a maximum of the *M*–*M* bond orders, and vice versa. The linear fit for the sums of the Pauling bond orders is much better; all 15 data points with the exception of *M*2 are very close to that trendline. The positive slope of the latter linear fit clearly shows that the 5*d* metal Hf prefers the positions with higher bond orders, compared to Zr. Hf forms stronger

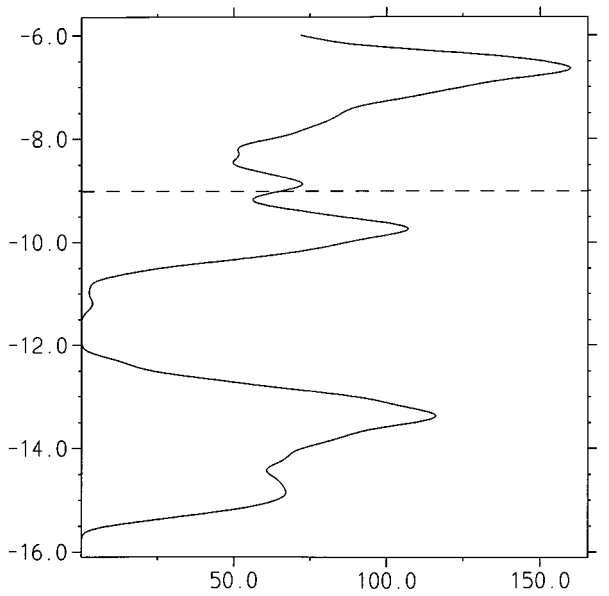

FIG. 2. Densities of states for hypothetical "$Hf_{14}P_9$." Dashed horizontal line represents Fermi level.

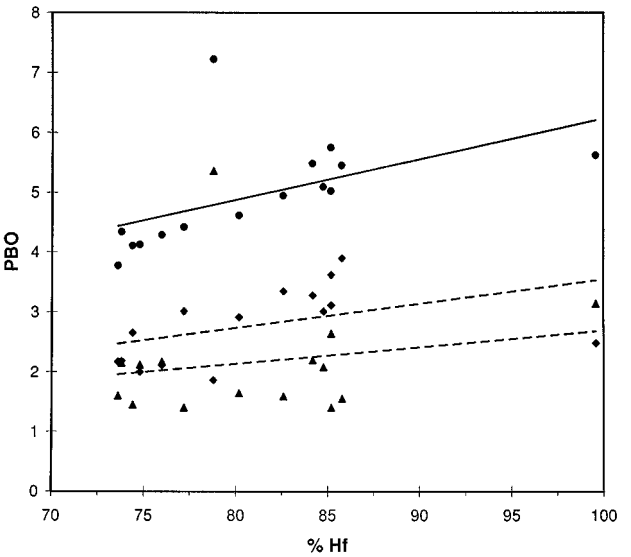

FIG. 3. Summed Pauling bond orders with varying Hf content for hypothetical "$Hf_{14}P_9$". Triangles: PBO(Hf–Hf); diamonds: PBO(Hf–P); circles: sum of PBO(Hf–Hf) and PBO(Hf–P) (total PBO). Lower dashed line: linear fit for the PBOs(Hf–Hf); upper dashed line: linear fit for the PBOs(Hf–P); solid line: linear fit for the total PBOs.

M–*M* bonds than Zr because of the greater expansion of the 5*d* orbitals and stronger *M*–P bonds because of the lower electronegativity. The good fit of the increase of the total bond orders with increasing Hf/Zr ratio indicates that in case of $Zr_{2.7}Hf_{11.3}P_9$ both kinds of interactions, *i.e.*, *M*–*M* and *M*–P, have similar importance for the differential site occupancies.

To confirm these results, we also calculated the sums of the Mulliken overlap populations using Hf parameters for all metal sites, as shown in arbitrary units in Fig. 4. The trends of Figs. 3 and 4 (shown in Table 5) are very similar, showing once more the good correlation between Mulliken overlap populations and Pauling bond orders. Again, the *M*2 site does not fit very well into the general trend of increasing bond order with increasing Hf/Zr ratio. According to the trendline of the sums of the Mulliken overlap population per *M* site, the Hf/Zr ratio should be highest, *i.e.*, equal to one, in case of *M*2. As discussed above, *M*2 is the only atom in the structure of $Zr_{2.7}Hf_{11.3}P_9$ with cubic *M* coordination. This might explain why the Hf/Zr ratio is lower than expected based on the total bond order of *M*2;

TABLE 5
Summed Pauling Bond Orders (PBO) and Mulliken Overlap Populations (MOP) for the 15 Metal Sites in Hypothetical "$Hf_{14}P_9$"

% *M*	*M* site	PBO(*M*–*M*)	PBO(*M*–P)	PBO, total	MOP(*M*–*M*)	MOP(*M*–P)	MOP, total
99.6(1.2)	1	3.14	2.48	5.62	1.975	1.37	3.345
85.8(1.0)	13	1.55	3.9	5.45	1.005	2.0625	3.0675
85.2(1.0)	14	2.64	3.11	5.75	1.365	1.755	3.12
85.2(1.0)	7	1.4	3.62	5.02	0.9825	2.0375	3.02
84.8(1.0)	10	2.08	3.01	5.09	1.3025	1.7425	3.045
84.2(1.0)	4	2.2	3.28	5.48	1.2325	1.84	3.0725
82.6(1.0)	9	1.59	3.35	4.94	1.1725	1.89	3.0625
80.2(1.0)	12	1.64	2.91	4.61	1.245	1.735	2.98
78.8(1.2)	2	5.36	1.86	7.22	2.21	0.99	3.2
77.2(1.0)	15	1.4	3.01	4.41	1.1725	1.795	2.9675
76.0(1.0)	3	2.17	2.11	4.28	1.485	1.38	2.865
74.8(1.0)	5	2.12	2	4.12	1.515	1.38	2.895
74.4(1.0)	6	1.45	2.65	4.1	1.27	1.685	2.955
73.8(1.0)	11	2.15	2.18	4.33	1.5825	1.315	2.8975
73.6(1.0)	8	1.6	2.17	3.77	1.3925	1.5175	2.91

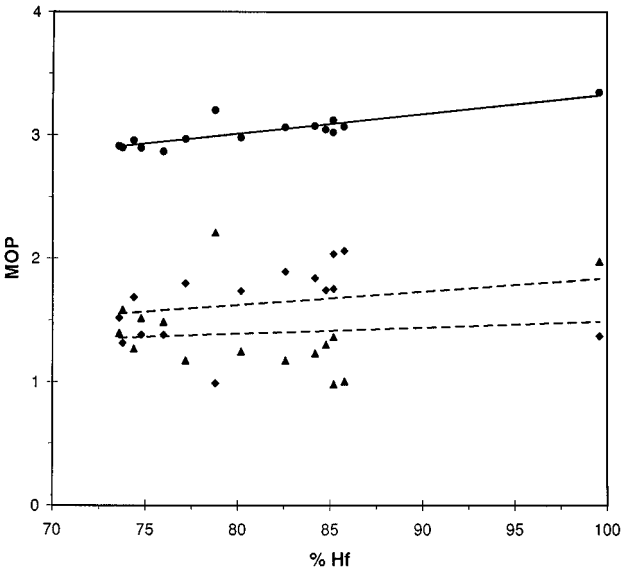

FIG. 4. Summed Mulliken overlap populations with varying Hf content for hypothetical "$Hf_{14}P_9$". Triangles: MOP(Hf–Hf); diamonds: MOP(Hf–P); circles: sum of MOP(Hf–Hf) and MOP(Hf–P) (total MOP). Lower dashed line: linear fit for the MOPs(Hf–Hf); upper dashed line: linear fit for the MOPs(Hf–P); solid line: linear fit for the total MOPs.

Zr generally has a higher preference for structures with *bcc* units, as can be seen by comparing different compounds with a similar metal/nonmetal ratio, for example $Zr_9Ni_2P_4$ and Hf_5NiP_3 (22), $Zr_{14}P_9$ and Hf_3P_2, and Zr_2S and Hf_2S (23).

ACKNOWLEDGMENTS

H.K. thanks the Deutsche Forschungsgemeinschaft for financial support of this work. The Ames Laboratory is operated for the U.S. Department of Energy by Iowa State University under Contract W-7405-Eng-82. This research was also supported by the Office of the Basic Energy Sciences, Materials Science Division, Department of Energy.

REFERENCES

1. X. Yao and H. F. Franzen, *J. Amer. Chem. Soc.* **113,** 1426 (1991).
2. X. Yao, G. J. Miller, and H. F. Franzen, *J. Alloys Compd.* **183,** 7 (1992).
3. X. Yao and H. F. Franzen, *J. Solid State Chem.* **86,** 88 (1990).
4. X. Yao and H. F. Franzen, *Z. Anorg. Allg. Chem.* **598/599,** 353 (1991).
5. G. A. Marking and H. F. Franzen, *Chem. Mater.* **5,** 678 (1993).
6. J. Cheng and H. F. Franzen, *J. Solid State Chem.* **121,** 362 (1996).
7. H. Kleinke and H. F. Franzen, *J. Amer. Chem. Soc.* **119,** 12824 (1997).
8. G. A. Marking and H. F. Franzen, *J. Alloys Compd.* **204,** L17 (1994).
9. L.-E. Tergenius, B. I. Noläng, and T. Lundström, *Acta Chem. Scand.* **A35,** 693 (1981).
10. X. Yao and H. F. Franzen, *J. Less-Common Met.* **142,** L27 (1988).
11. X. Yao, G. A. Marking, and H. F. Franzen, *Ber. Bunsenges. Phys. Chem.* **96,** 1152 (1992).
12. H. Kleinke and H. F. Franzen, *Inorg. Chem.* **35,** 5272 (1996).
13. TEXSAN: Single Crystal Structure Analysis Software, Version 5.0, Molecular Structure Corporation, The Woodlands, TX, 1989.
14. P. Villars and L. D. Calvert, "Pearson's Handbook of Crystallographic Data for Intermetallic Phases." ASM International, Materials Park, OH, 1991.
15. H. Kleinke and H. F. Franzen, *Acta Crystallogr. Sect. C* **52,** 2127 (1996).
16. L. Pauling, "The Nature of the Chemical Bond," 3rd ed. Cornell University Press, Ithaca, 1948.
17. R. Hoffmann, *J. Chem. Phys.* **39,** 1397 (1963).
18. M.-H. Whangbo and R. Hoffmann, *J. Am. Chem. Soc.* **100,** 6093 (1978).
19. H. Kleinke and H. F. Franzen, *Angew. Chem. Int. Ed. Engl.* **35,** 1934 (1996).
20. E. Clementi and C. Roetti, *Atomic Data and Nuclear Data Tables* **14,** 177 (1974).
21. H. F. Franzen and M. Köckerling, *Prog. Solid St. Chem.* **23,** 265 (1995).
22. H. Kleinke and H. F. Franzen, *Chem. Mater.* **9,** 1030 (1997).
23. H. F. Franzen and J. Graham, *Z. Kristallogr.* **123,** 133 (1966).